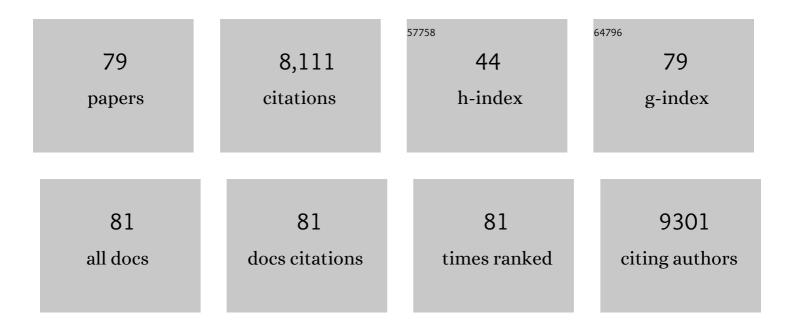
List of Publications by Year in descending order

Source: https://exaly.com/author-pdf/3418272/publications.pdf Version: 2024-02-01



VIIN KUANC

| #  | Article   | IF   | CITATIONS |
|----|---|------|-----------|
| 1  | First-principles study of the oxygen evolution reaction on Ni3Fe-layered double hydroxides surfaces with varying sulfur coverage. Molecular Catalysis, 2022, 519, 112116.   | 2.0  | 1         |
| 2  | 3D printed hierarchical spinel monolithic catalysts for highly efficient semi-hydrogenation of acetylene. Nano Research, 2022, 15, 6010-6018.   | 10.4 | 8         |
| 3  | Layered double hydroxide-based electrocatalysts for the oxygen evolution reaction: identification<br>and tailoring of active sites, and superaerophobic nanoarray electrode assembly. Chemical Society<br>Reviews, 2021, 50, 8790-8817. | 38.1 | 331       |
| 4  | Selective and High Current CO <sub>2</sub> Electro-Reduction to Multicarbon Products in Near-Neutral KCl Electrolytes. Journal of the American Chemical Society, 2021, 143, 3245-3255.  | 13.7 | 108       |
| 5  | Rare-earth-regulated Ru-O interaction within the pyrochlore ruthenate for electrocatalytic oxygen evolution in acidic media. Science China Materials, 2021, 64, 1653-1661.  | 6.3  | 27        |
| 6  | Iridium in Tungsten Trioxide Matrix as an Efficient Biâ€Functional Electrocatalyst for Overall Water<br>Splitting in Acidic Media. Small, 2021, 17, e2102078.   | 10.0 | 28        |
| 7  | MoSx microgrid electrodes with geometric jumping effect for enhancing hydrogen evolution efficiency. Science China Materials, 2021, 64, 892-898.  | 6.3  | 3         |
| 8  | A multiphase nickel iron sulfide hybrid electrode for highly active oxygen evolution. Science China<br>Materials, 2020, 63, 356-363.  | 6.3  | 23        |
| 9  | Synthesis and Properties of Stable Sub-2-nm-Thick Aluminum Nanosheets: Oxygen Passivation and<br>Two-Photon Luminescence. CheM, 2020, 6, 448-459.   | 11.7 | 15        |
| 10 | An Artificial Electrode/Electrolyte Interface for CO <sub>2</sub> Electroreduction by Cation<br>Surfactant Selfâ€Assembly. Angewandte Chemie - International Edition, 2020, 59, 19095-19101.  | 13.8 | 71        |
| 11 | An Artificial Electrode/Electrolyte Interface for CO <sub>2</sub> Electroreduction by Cation<br>Surfactant Selfâ€Assembly. Angewandte Chemie, 2020, 132, 19257-19263.   | 2.0  | 45        |
| 12 | Understanding of Dynamic Contacting Behaviors of Underwater Gas Bubbles on Solid Surfaces.<br>Langmuir, 2020, 36, 11422-11428.  | 3.5  | 7         |
| 13 | Antibuoyancy and Unidirectional Gas Evolution by Janus Electrodes with Asymmetric Wettability. ACS<br>Applied Materials & Interfaces, 2020, 12, 23627-23634.  | 8.0  | 29        |
| 14 | Microwave chemistry, recent advancements, and eco-friendly microwave-assisted synthesis of nanoarchitectures and their applications: a review. Materials Today Nano, 2020, 11, 100076.  | 4.6  | 154       |
| 15 | Electroreduction of CO <sub>2</sub> to Formate on a Copper-Based Electrocatalyst at High Pressures with High Energy Conversion Efficiency. Journal of the American Chemical Society, 2020, 142, 7276-7282.                              | 13.7 | 165       |
| 16 | Recent Advances in Nonâ€Precious Metalâ€Based Electrodes for Alkaline Water Electrolysis.<br>ChemNanoMat, 2020, 6, 336-355.   | 2.8  | 92        |
| 17 | Common-Ion Effect Triggered Highly Sustained Seawater Electrolysis with Additional NaCl<br>Production. Research, 2020, 2020, 2872141.   | 5.7  | 28        |
| 18 | Zn Doped NiMn-Layered Double Hydroxide for High Performance Ni–Zn Battery. Journal of the<br>Electrochemical Society, 2020, 167, 160550.  | 2.9  | 4         |

| #  | Article  | IF   | CITATIONS |
|----|--|------|-----------|
| 19 | Hierarchical cobalt oxide@Nickel-vanadium layer double hydroxide core/shell nanowire arrays with<br>enhanced areal specific capacity for nickel–zinc batteries. Journal of Power Sources, 2019, 436, 226867.                   | 7.8  | 48        |
| 20 | A safe and non-flammable sodium metal battery based on an ionic liquid electrolyte. Nature<br>Communications, 2019, 10, 3302.  | 12.8 | 173       |
| 21 | Amorphous Rutheniumâ€6ulfide with Isolated Catalytic Sites for Ptâ€Like Electrocatalytic Hydrogen<br>Production Over Whole pH Range. Small, 2019, 15, e1904043.  | 10.0 | 71        |
| 22 | Hydrogen Production: Amorphous Rutheniumâ€Sulfide with Isolated Catalytic Sites for Ptâ€Like<br>Electrocatalytic Hydrogen Production Over Whole pH Range (Small 46/2019). Small, 2019, 15, 1970249.                            | 10.0 | 0         |
| 23 | Constructing Earthâ€abundant 3D Nanoarrays for Efficient Overall Water Splitting – A Review.<br>ChemCatChem, 2019, 11, 1550-1575.  | 3.7  | 108       |
| 24 | Superaerophilic copper nanowires for efficient and switchable CO <sub>2</sub> electroreduction.<br>Nanoscale Horizons, 2019, 4, 490-494.   | 8.0  | 39        |
| 25 | Engineering Interfacial Aerophilicity of Nickel-Embedded Nitrogen-Doped CNTs for Electrochemical CO <sub>2</sub> Reduction. ACS Applied Energy Materials, 2019, 2, 3991-3998.  | 5.1  | 23        |
| 26 | Enhancing oxygen evolution reaction by cationic surfactants. Nano Research, 2019, 12, 2302-2306.   | 10.4 | 28        |
| 27 | Synthesis and performance optimization of ultrathin two-dimensional CoFePt alloy materials <i>via in situ</i> topotactic conversion for the hydrogen evolution reaction. Journal of Materials Chemistry A, 2019, 7, 9517-9522. | 10.3 | 17        |
| 28 | Solar-driven, highly sustained splitting of seawater into hydrogen and oxygen fuels. Proceedings of the United States of America, 2019, 116, 6624-6629.  | 7.1  | 524       |
| 29 | A general route <i>via</i> formamide condensation to prepare atomically dispersed<br>metal–nitrogen–carbon electrocatalysts for energy technologies. Energy and Environmental Science,<br>2019, 12, 1317-1325.                 | 30.8 | 290       |
| 30 | Morphology effects of bismuth catalysts on electroreduction of carbon dioxide into formate.<br>Electrochimica Acta, 2019, 305, 388-393.  | 5.2  | 34        |
| 31 | Boosting oxygen evolution of single-atomic ruthenium through electronic coupling with cobalt-iron layered double hydroxides. Nature Communications, 2019, 10, 1711.  | 12.8 | 446       |
| 32 | An electrodeposition approach to metal/metal oxide heterostructures for active hydrogen evolution catalysts in near-neutral electrolytes. Nano Research, 2019, 12, 1431-1435.  | 10.4 | 31        |
| 33 | Breaking the symmetry: Gradient in NiFe layered double hydroxide nanoarrays for efficient oxygen<br>evolution. Nano Energy, 2019, 60, 661-666.   | 16.0 | 52        |
| 34 | Highly active oxygen evolution integrated with efficient CO <sub>2</sub> to CO electroreduction.<br>Proceedings of the National Academy of Sciences of the United States of America, 2019, 116, 23915-23922.                   | 7.1  | 58        |
| 35 | NiFe Hydroxide Lattice Tensile Strain: Enhancement of Adsorption of Oxygenated Intermediates for<br>Efficient Water Oxidation Catalysis. Angewandte Chemie, 2019, 131, 746-750.  | 2.0  | 55        |
| 36 | Selectivity regulation of CO2 electroreduction through contact interface engineering on superwetting Cu nanoarray electrodes. Nano Research, 2019, 12, 345-349.  | 10.4 | 80        |

| #  | Article   | IF   | CITATIONS |
|----|---|------|-----------|
| 37 | NiFe Hydroxide Lattice Tensile Strain: Enhancement of Adsorption of Oxygenated Intermediates for<br>Efficient Water Oxidation Catalysis. Angewandte Chemie - International Edition, 2019, 58, 736-740.            | 13.8 | 335       |
| 38 | Janus electrode with simultaneous management on gas and liquid transport for boosting oxygen reduction reaction. Nano Research, 2019, 12, 177-182.  | 10.4 | 43        |
| 39 | Tuning Electronic Structure of NiFe Layered Double Hydroxides with Vanadium Doping toward High<br>Efficient Electrocatalytic Water Oxidation. Advanced Energy Materials, 2018, 8, 1703341.                        | 19.5 | 505       |
| 40 | Understanding the incorporating effect of Co2+/Co3+ in NiFe-layered double hydroxide for electrocatalytic oxygen evolution reaction. Journal of Catalysis, 2018, 358, 100-107.                                    | 6.2  | 194       |
| 41 | Layered double hydroxides with atomic-scale defects for superior electrocatalysis. Nano Research, 2018, 11, 4524-4534.  | 10.4 | 130       |
| 42 | Singleâ€Crystalline Ultrathin Co <sub>3</sub> O <sub>4</sub> Nanosheets with Massive Vacancy Defects for Enhanced Electrocatalysis. Advanced Energy Materials, 2018, 8, 1701694.                                  | 19.5 | 451       |
| 43 | NiCoFeâ€Layered Double Hydroxides/Nâ€Doped Graphene Oxide Array Colloid Composite as an Efficient<br>Bifunctional Catalyst for Oxygen Electrocatalytic Reactions. Advanced Energy Materials, 2018, 8,<br>1701905. | 19.5 | 276       |
| 44 | Effects of redox-active interlayer anions on the oxygen evolution reactivity of NiFe-layered double<br>hydroxide nanosheets. Nano Research, 2018, 11, 1358-1368.  | 10.4 | 134       |
| 45 | Boosting oxygen reaction activity by coupling sulfides for high-performance rechargeable metal–air<br>battery. Journal of Materials Chemistry A, 2018, 6, 21162-21166.  | 10.3 | 38        |
| 46 | Introducing Fe <sup>2+</sup> into Nickel–Iron Layered Double Hydroxide: Local Structure Modulated<br>Water Oxidation Activity. Angewandte Chemie, 2018, 130, 9536-9540.   | 2.0  | 86        |
| 47 | Introducing Fe <sup>2+</sup> into Nickel–Iron Layered Double Hydroxide: Local Structure Modulated<br>Water Oxidation Activity. Angewandte Chemie - International Edition, 2018, 57, 9392-9396.                    | 13.8 | 284       |
| 48 | Bright quantum dots emitting at â^¼1,600 nm in the NIR-IIb window for deep tissue fluorescence imaging.<br>Proceedings of the National Academy of Sciences of the United States of America, 2018, 115, 6590-6595. | 7.1  | 310       |
| 49 | Phosphorus oxoanion-intercalated layered double hydroxides for high-performance oxygen evolution. Nano Research, 2017, 10, 1732-1739.   | 10.4 | 139       |
| 50 | Topotactic reduction of layered double hydroxides for atomically thick two-dimensional non-noble-metal alloy. Nano Research, 2017, 10, 2988-2997.   | 10.4 | 38        |
| 51 | Single Crystalline Ultrathin Nickel–Cobalt Alloy Nanosheets Array for Direct Hydrazine Fuel Cells.<br>Advanced Science, 2017, 4, 1600179.   | 11.2 | 104       |
| 52 | Superaerophobic Ultrathin Ni–Mo Alloy Nanosheet Array from In Situ Topotactic Reduction for<br>Hydrogen Evolution Reaction. Small, 2017, 13, 1701648.   | 10.0 | 190       |
| 53 | Unconventional Carbon: Alkaline Dehalogenation of Polymers Yields Nâ€Doped Carbon Electrode for<br>Highâ€Performance Capacitive Energy Storage. Advanced Functional Materials, 2016, 26, 3340-3348.               | 14.9 | 95        |
| 54 | Probing the seeded protocol for high-concentration preparation of silver nanowires. Nano Research, 2016, 9, 1532-1542.  | 10.4 | 25        |

| #  | Article  | IF   | CITATIONS |
|----|--|------|-----------|
| 55 | ZnO-promoted dechlorination for hierarchically nanoporous carbon as superior oxygen reduction electrocatalyst. Nano Energy, 2016, 26, 241-247.   | 16.0 | 72        |
| 56 | Universal Parameter Optimization of Density Gradient Ultracentrifugation Using CdSe Nanoparticles<br>as Tracing Agents. Analytical Chemistry, 2016, 88, 8495-8501.   | 6.5  | 11        |
| 57 | Amorphous Co–Mo–S ultrathin films with low-temperature sulfurization as high-performance<br>electrocatalysts for the hydrogen evolution reaction. Journal of Materials Chemistry A, 2016, 4,<br>13731-13735. | 10.3 | 48        |
| 58 | Ternary NiCoP nanosheet arrays: An excellent bifunctional catalyst for alkaline overall water splitting. Nano Research, 2016, 9, 2251-2259.  | 10.4 | 342       |
| 59 | High-Performance Water Electrolysis System with Double Nanostructured Superaerophobic<br>Electrodes. Small, 2016, 12, 2492-2498.   | 10.0 | 113       |
| 60 | Singleâ€Crystalline Ultrathin Nickel Nanosheets Array from Inâ€Situ Topotactic Reduction for Active and<br>Stable Electrocatalysis. Angewandte Chemie - International Edition, 2016, 55, 693-697.            | 13.8 | 225       |
| 61 | Superior anti-CO poisoning capability: Au-decorated PtFe nanocatalysts for high-performance methanol oxidation. Chemical Communications, 2016, 52, 3903-3906.  | 4.1  | 57        |
| 62 | Characterization of exosomes derived from ovarian cancer cells and normal ovarian epithelial cells by nanoparticle tracking analysis. Tumor Biology, 2016, 37, 4213-4221.                                    | 1.8  | 74        |
| 63 | Development of hydrophilicity gradient ultracentrifugation method for photoluminescence investigation of separated non-sedimental carbon dots. Nano Research, 2015, 8, 2810-2821.                            | 10.4 | 49        |
| 64 | Rational design of graphene oxide and its hollow CoO composite for superior oxygen reduction reaction. Science China Materials, 2015, 58, 534-542.   | 6.3  | 30        |
| 65 | Separation of colloidal two dimensional materials by density gradient ultracentrifugation. Journal of Solid State Chemistry, 2015, 224, 120-126.   | 2.9  | 7         |
| 66 | Controllable Assembly and Separation of Colloidal Nanoparticles through a Oneâ€Tube Synthesis Based on Density Gradient Centrifugation. Chemistry - A European Journal, 2015, 21, 7211-7216.                 | 3.3  | 11        |
| 67 | Single-crystalline dendritic bimetallic and multimetallic nanocubes. Chemical Science, 2015, 6, 7122-7129.   | 7.4  | 61        |
| 68 | Three-dimensional porous superaerophobic nickel nanoflower electrodes for high-performance hydrazine oxidation. Nano Research, 2015, 8, 3365-3371.   | 10.4 | 70        |
| 69 | Hierarchically porous indium oxide nanolamellas with ten-parts-per-billion-level<br>formaldehyde-sensing performance. Sensors and Actuators B: Chemical, 2015, 206, 714-720.                                 | 7.8  | 31        |
| 70 | Ultrathin branched PtFe and PtRuFe nanodendrites with enhanced electrocatalytic activity. Journal of Materials Chemistry A, 2015, 3, 1182-1187.  | 10.3 | 65        |
| 71 | Solvent switching and purification of colloidal nanoparticles through water/oil Interfaces within a density gradient. Nano Research, 2014, 7, 1670-1679.   | 10.4 | 8         |
| 72 | Ultrathin Dendritic Pt <sub>3</sub> Cu Triangular Pyramid Caps with Enhanced Electrocatalytic<br>Activity. ACS Applied Materials & Interfaces, 2014, 6, 17748-17752.   | 8.0  | 69        |

| #  | Article   | IF   | CITATIONS |
|----|---|------|-----------|
| 73 | Solvothermal synthesis of FeCo nanoparticles for magneto-controllable biocatalysis. RSC Advances, 2014, 4, 11136-11141.   | 3.6  | 9         |
| 74 | Synthesis Mechanism Study of Layered Double Hydroxides Based on Nanoseparation. Inorganic<br>Chemistry, 2013, 52, 8694-8698.  | 4.0  | 24        |
| 75 | Highly controlled bifunctional Ag@rubrene core–shell nanostructures: surface-enhanced fluorescence and Raman scattering. Journal of Materials Chemistry C, 2013, 1, 4146.                     | 5.5  | 12        |
| 76 | Mesoporous assembled SnO2 nanospheres: Controlled synthesis, structural analysis and ethanol sensing investigation. Sensors and Actuators B: Chemical, 2013, 181, 629-636.                    | 7.8  | 21        |
| 77 | Ultrashort Single-Walled Carbon Nanotubes: Density Gradient Separation, Optical Property, and Mathematical Modeling Study. Journal of Physical Chemistry C, 2012, 116, 24770-24776.           | 3.1  | 18        |
| 78 | Understanding the "Tailoring Synthesis―of CdS Nanorods by O <sub>2</sub> . Inorganic Chemistry, 2012, 51, 1302-1308.  | 4.0  | 16        |
| 79 | Experimental and Mathematical Modeling Studies of the Separation of Zinc Blende and Wurtzite<br>Phases of CdS Nanorods by Density Gradient Ultracentrifugation. ACS Nano, 2011, 5, 3242-3249. | 14.6 | 35        |